Published in final edited form as:
Biochemistry. 2012 April 3; 51(13): 2670–2683. doi:10.1021/bi2015162.

Analysis of the Inhibition and Remodeling of Islet Amyloid Polypeptide Amyloid Fibers by Flavanols

Ping Cao and **Daniel P. Raleigh***
Department of Chemistry, Stony Brook University, Nicolls Road Stony Brook, NY 11794-3400

Abstract

Islet amyloid polypeptide (IAPP, amylin) is responsible for amyloid formation in type 2 diabetes and in transplanted islets. The flavanol, (−)-Epigallocatechin-3-gallate [EGCG; (2*R*,3*R*)-5,7-dihydroxy-2-(3,4,5-trihydroxyphenyl)-3,4-dihydro-2*H*-1-benzopyran-3-yl3,4,5-trihydroxybenzoate] is an effective inhibitor of amyloid formation by IAPP, however, the interactions required for the inhibition of IAPP amyloid formation and for the remodeling of amyloid fibers are not known. A range of features have been proposed to be critical for EGCG protein interactions, including interactions with aromatic residues, interactions with amino groups, or sulfhydryls. Using a set of IAPP analogs we show that none of these are required. Studies in which EGCG is added to the lag phase of amyloid formation suggest that it interacts with intermediates as well as with monomers and amyloid. The features of EGCG required for effective inhibition were examined. The stereoisomer of EGCG, (−)-Gallocatechin gallate (GCG), is an effective inhibitor, although less so than EGCG. Removing the gallate ester moiety leads to EGC which is a less effective inhibitor. Removing only the 3-hydroxyl group of the tri-hydroxyphenyl ring leads to a compound which has more pronounced effects on the lag phase than EGC, but is less effective at reducing the amount of amyloid. Elimination of both the 3-hydroxy group and the gallate ester results in loss of activity. EGCG remodels IAPP amyloid fibers, but does not fully resolubilize them to unstructured monomers and the remodeling is not the reverse of amyloid assembly. The ability of the compounds to remodel IAPP amyloid closely follows their relative ability to inhibit amyloid formation.

Keywords

Amylin; Amyloid Inhibitors; Islet Amyloid; Polypeptide; Epigallocatechin 3-gallate; EGCG

Amyloid formation plays a critical role in a more than 25 different human diseases including Huntington's disease, Parkinson's disease, Alzheimer's disease, the transmissible spongiform encephalopathies and type-2 diabetes (1–3). The search for inhibitors of amyloid fiber formation is an active area of research and particular attention has been focused on

*To whom correspondence should be addressed: D.P.R. Phone: 631-632-9547, Fax: 631-632-7960, draleigh@notes.cc.sunysb.edu.

SUPPORTING INFORMATION AVAILABLE

Figures showing that the presence of thioflavin-T does not influence the kinetics of IAPP amyloid formation at the concentration used here and does not interfere with inhibition assays. Additional TEM images of IAPP recorded after the addition of EGCG at various time points. A figure showing that EGCG inhibits IAPP amyloid formation for at least 140 hours. A figure showing the effects of adding a substoichiometric amount of EGCG at different time points during amyloid formation by IAPP. Thioflavin-T kinetic curves and TEM images demonstrating that EGCG inhibits amyloid formation by F15L, F23L-IAPP and $IAPP_{AC8-24}$ and remodels amyloid fibers formed by both polypeptides. Figures comparing the effectiveness of the compounds when they are added at a five fold excess relative to IAPP. A figure comparing the rate of remodeling of IAPP amyloid fibers after the addition of EGCG during the growth phase and in the plateau region. A summary table of the solubility studies. A figure showing the effect of adding additional EGCG after a remodeling reaction has apparently reached completion. This information is available free of charge via the Internet at http://pubs.acs.org.

flavanols (4–15). Among the most potent inhibitors found to date is the ester of epigallocatechin and gallic acid, (−)-Epigallocatechin 3-Gallate [EGCG; (2*R*,3*R*)-5,7-dihydroxy-2-(3,4,5-trihydroxyphenyl)-3,4-dihydro-2*H*-1-benzopyran-3-yl 3,4,5-trihydroxybenzoate]. EGCG is the most abundant biologically active compound in green tea and inhibits amyloid formation *in vitro* by a range of natively unfolded polypeptides including islet amyloid polypeptide, (IAPP, also known as Amylin), Aβ, α-synuclein, the AIDs enhancer factor SEVI, and the surface protein from *Plasmodium falcipran merozite*. The compound has also been shown to induce conversion of the cellular form of the prion protein into a form which differs from the pathological scrapie prion protein conformation (16–23). EGCG is thought to bind to unaggregated polypeptides and redirect the pathway of amyloid formation to off-pathway non-toxic oligomers (16), although this appears not to be the case for at least one protein (24). A different polyphenol, exifone [3,4,5,2',3',4'-hexahydroxybenzophenone [(2,3,4-trihydroxyphenyl)-(3,4,5-trihydroxyphenyl) methanone]], has been shown to function by a different mechanism that involves trapping on-pathway intermediates (25). Irrespective of the mechanistic details, EGCG inhibits a very broad range of amyloidogenic polypeptide, and its mode of action is of considerable interest. The ability of EGCG to remodel amyloid fibers has been examined for fewer polypeptides, but it has been shown to remodel the fibers formed by Aβ, IAPP and α-synuclein into non-fibril material (20, 22).

The details of the interactions between EGCG or other flavanols and target polypeptides are not yet well understood, but a range of interactions have been proposed to be important; including interactions between the compounds and aromatic residues, interactions with amino groups, or with Cys residues (10, 12, 23, 26–28). Structure activity studies of derivatives of EGCG are relatively few and, to the best of our knowledge, those which have been reported have largely examined the remodeling of amyloid rather than the kinetics of amyloid formation (22).

Here we focus on the inhibition of amyloid formation by IAPP and the remodeling of IAPP amyloid. IAPP is the causative agent of islet amyloid in type-2 diabetes. The molecule is a 37 residue polypeptide hormone which contains a disulfide and an amidated C-terminus (Figure-1). IAPP has been identified in all mammalian species examined and is a member of the calcitonin-like family of peptides, which include calcitonin, adrenomedullin, and calcitonin gene-related peptide (29–32). The hormone is secreted in response to the same stimuli that lead to insulin secretion and normally functions as an endocrine partner to insulin (31, 33–34), but forms islet amyloid in type-2 diabetes (29–30, 33, 35–41). The polypeptide is one of the most amyloidogenic polypeptides known and synthetic aggregates of human IAPP are toxic to pancreatic β-cells, arguing that the process of IAPP amyloid fibril formation may contribute to islet cell death in type 2 diabetes (36–39, 41–42). Islet amyloid formation also plays an important role in the loss of islet cell grafts following islet transplantation (43–45). Hence there is considerable interest in developing and characterizing inhibitors of IAPP amyloid formation.

MATERIAL AND METHODS

EGCG, EGC, ECG, GCG, Catechin, and Epi-Catechin were purchased from Sigma-Aldrich. Stock solutions of the compounds were prepared immediately before use.

Peptide Synthesis and Purification

Human IAPP, and IAPP mutants (Figure-1) were synthesized on a 0.25 mmol scale using an Applied Biosystems 433A peptide synthesizer, by 9-fluornylmethoxycarbonyl (Fmoc) chemistry. Pesudoprolines were incorporated to facilitate the synthesis. 5-(4'-fmoc-aminomethyl-3',5-dimethoxyphenol) valeric acid (PAL-PEG) resin was used to afford an

amidated C-terminus (46). The peptide was cleaved from the resin using standard TFA protocols. Crude peptides were oxidized by dimethyl sulfoxide (DMSO) (47). The peptides were purified by reverse-phase HPLC using a Vydac C18 preparative column with HCl as the counter-ion since the presence of TFA has been shown to affect amyloid formation by some IAPP derived peptides (48). After the initial purification, the peptide was washed with cold ether, centrifuged, dried and then redissolved in HFIP and subjected to a second round of HPLC purification. This procedure was necessary to remove residual scavengers. Analytical HPLC was used to check the purity of the peptide. The identity of the pure peptides was confirmed by mass spectrometry using a Bruker MALDI-TOF MS; IAPP observed 3904.6, expected 3904.8; 3XL-IAPP, observed 3785.8, expected 3786.2; F15L, F23L-IAPP, observed 3835.8, expected 3836.2; $IAPP_{Ac8-37}$, observed 3225.1, expected 3225.4; $IAPP_{Ac8-24}$ observed 1917.2, expected 1917.0.

Sample Preparation for in vitro Biophysical Assays of Amyloid Formation

Stock solutions (1.60 mM) of IAPP were prepared in 100% hexafluoroisopropyl alcohol (HFIP) and stored at −20°C. Aliquots of IAPP peptide in HFIP were filtered through a 0.22 μm filter and freeze-dried. A Tris-HCl buffered (20 mM, pH 7.4) thioflavin-T solution was added to these samples to initiate amyloid formation.

Thioflavin-T Fluorescence Assays

Fluorescence measurements were performed using a Beckman model D880 plate reader. An excitation wavelength of 430 nm and emission wavelength of 485 nm were used for the thioflavin-T studies. The samples were incubated at 25°C in 96-well plates. An excitation filter of 430 nm and an emission filter of 485 nm were used. All solutions for these studies were prepared by adding a Tris-HCl buffered (20 mM, pH 7.4) thioflavin-T solution to IAPP peptide (in lyophilized dry form) immediately before the measurement. The final concentration was 16 μM or 32 μM peptide and 32 μM thioflavin-T with or without flavanols in 20 mM Tris-HCl. For the comparative studies of EGCG, ECG, EGC, GCG, Catehchin, and Epi-Catehchin, 0.25% DMSO was present in the solution. EGCG is very soluble in water, (20 mg/ml), as were all of the derivatives except for ECG. Thus a concentrated stock solution of ECG was prepared in DMSO and diluted into buffer. The final DMSO concentration was 0.25%. Similar conditions were used for the other derivatives, for consistency.

Transmission Electron Microscopy (TEM)

TEM was performed at the Life Science Microscopy Center at the Stony Brook University. TEM samples were prepared from the solutions used for the fluorescence measurements. 15 μL of the peptide solution was removed at the end of the kinetic runs and blotted on a carbon-coated Formvar 300 mesh copper grid for 1 min and then negatively stained with saturated uranyl acetate for 1 min.

IAPP Solubility Measurements

The soluble fraction of IAPP was measured using solutions that had been centrifuged to remove fibril material and high molecular weight aggregates. The concentration of soluble peptide was determined using the Bradford assay. Control experiments were conducted using BSA standards in the presence and absence of EGCG. The presence of EGCG affected the measured absorbance by less than 3.8%. The amount of soluble protein was measured for a freshly dissolved sample of IAPP and the amount remaining in solution after amyloid formation was determined by centrifuging the sample at 20,000 g, 25°C for 30 min using a Beckman Coulter bench top Microfuge 22R centrifuge. The upper 100 μl of the supernatant was used for quantification. The Bradford assay was used to measure the amount of soluble

peptide and was performed in 96-well plates using a Beckman model D880 plate reader. 100 μl of dye reagent was added to a 100 μl sample solution and the absorbance was measured at 595 nm after 30 seconds of linear shaking and 2 minutes incubation. Absorbance readings were calibrated with a standard series of human IAPP peptide that was freshly dissolved in water and was quantified by measuring the absorption at 280 nm. The molar extinction coefficient used was 1615 $M^{-1}cm^{-1}$.

A set of experiments with and without EGCG were conducted. Experiments were conducted with samples to which EGCG (16 μM) had been added at time=0. The amount of soluble IAPP was measured at time=0 and time=50 hrs. Control studies were also performed with samples of IAPP in the absence of EGCG. Solubility experiments were also conducted on samples that had been remodeled by EGCG. 16 μM human IAPP was incubated at 25°C in 20 mM pH 7.4 Tris-HCl buffer to form amyloid fibrils. 50 hours later, EGCG was added to the fiber solution. After incubation for another 45 hours (i.e. 95 hours after the reaction was initiated), the amount of soluble protein was measured.

Results and Discussion

The primary sequence of IAPP is shown in Figure 1 together with the IAPP analogs studied here. The 3XL-IAPP variant is a triple mutant in which each aromatic residue has been replaced by Leu. 3XL-IAPP forms amyloid fibers which are similar to those of wild type IAPP although a bit thinner. The mutant allows us to test the role of the C-terminal tyrosine as well as the role of the other aromatic residues (49). The F15L, F23L peptide lacks the two Phe residues in wild type IAPP and allows us to test the importance of potential drug Phe interactions. In order to study the potential importance of protein amino groups we prepared two acetylated analogs of IAPP. The first includes residues 8–37 (with an acetylated N-terminus) and is denoted $IAPP_{Ac8\text{-}37}$. This peptide forms amyloid fibers on a time scale similar to wild type IAPP and generates fibers with the same morphology as wild type (50). The second is comprised of residues 8–24, again with an acetylated N-terminus, (denoted $IAPP_{Ac8\text{-}24}$). Both of these peptides lack free amino groups. Figure-1 also displays the structure of EGCG and the derivatives studied here. GCG is the stereoisomer of EGCG. ECG is similar in structure to EGCG but lacks the 5-hydroxyl group on the tri-hydroxyl ring. EGC includes the 5-hydroxyl group, but lacks the gallate ester. Comparative analysis of EGC and EGCG allows an assessment of role of the gallate ester. Catechin and its stereoisomer, Epi-Catechin, lack both the gallate ester group and the 5-hydroxyl group of the tri hydroxyl group. Historically, they were the first compounds in this class to be characterized as potential inhibitors of β-sheet linked polymerization. Early studies using model homo-polymers of amino acids showed that the catechins inhibit the coil to β-sheet transition (51).

Amyloid formation by IAPP displays a lag phase during which no detectable amyloid fibrils are formed followed by a growth phase which leads to a steady state in which amyloid fibrils are in equilibrium with soluble peptide. The rate of amyloid formation by IAPP was measured in the presence and in the absence of flavanols using thioflavin-T binding assays. The dye is believed to bind to the groves formed on the surface of amyloid fibers by the in-register alignment of side chains in the cross β-sheet structure. Binding of the dye reduces self-quenching by restricting the rotation of the benzothiozole and benzaminic rings, and the fluorescent quantum yield of the probe increases when it binds to amyloid fibrils (52). Thioflavin-T is not completely amyloid specific and it is important to validate its use on the system of interest. Previous studies, which made use of the fluorescent amino acid *p*-cyanophenylalanine, have shown that thioflavin-T experiments accurately report on the kinetics of IAPP amyloid formation and do not alter the observed rate of aggregation (53). There can also be complications with thioflavin-T studies of amyloid inhibition; compounds

which appear to be inhibitors in thioflavin-T assays may do so because they inhibit thioflavin-T binding to fibrils or quench the fluorescence of bound thioflavin-T rather than inhibit amyloid formation (15, 54). This can be problematic for some flavanols and related compounds, although not for EGCG (55). Nonetheless, we confirmed the results of all thioflavin-T binding assays using transmission electron microscopy (TEM).

EGCG inhibits amyloid formation by IAPP when added in the lag phase or in the growth phase

The mechanism of amyloid formation by IAPP is not known, but a number of groups have proposed that population of helical intermediates could be important (56–59). Structural studies of a fusion of IAPP with Maltose binding protein support this conjecture as do NMR and CD experiments and studies of rationally designed peptide inhibitors are consistent with this model (58–61). Mass spectroscopy studies have revealed the rapid formation of low order oligomers during IAPP amyloid formation (62) and a number of studies have utilized TEM to reveal the presence of non-fibril material in the lag phase. EGCG is known to inhibit amyloid formation by IAPP and a range of other polypeptides when it is added at the start of an amyloid reaction and it has been shown to remodel some preformed amyloid fibers into oligomeric species, but it is not known if it effectively interacts with species populated during the assembly of IAPP amyloid fibers. Thus, we examined the effect of adding EGCG at different time points after amyloid formation commenced.

We first conducted control experiments to test if the presence of thioflavin-T influences the results of our inhibition assays. It does not. IAPP readily forms amyloid in the absence of thioflavin-T and EGCG is still a highly effective inhibitor. Additional control experiments reveal that the time course of IAPP amyloid formation is independent of the ratio of thioflavin-T to IAPP over the range tested, and EGCG is a very effective inhibitor under these conditions (Supporting Information).

If EGCG were only able to bind to initially populated species, we would expect to see less effect when the compound is added in the middle or at the end of the lag phase relative to what is observed when it is added at time=0. EGCG is still effective if is added in the lag phase or at the end of the lag phase. Thioflavin-T monitored kinetic progress curves for IAPP in the presence and absence of EGCG are displayed in Figure-2. The curve measured in the absence of EGCG is typical of that observed for IAPP *in vitro*. The TEM image of the sample without inhibitor revealed extensive amyloid deposits. If EGCG is added at time=0, no change in thioflavin-T fluorescence is observed over the course of the reaction and no fibers are observed by TEM, in agreement with previous studies (Figure-2, Supporting Information) (20). TEM analysis of a sample removed in the middle of the lag phase, before the addition of EGCG shows some small spherical objects and very short fiber-like material (Figure-2B). We added EGCG at this point and, waited another 43 hours, (50 hours total after initiation of amyloid formation), and then recorded a TEM image. Small amounts of thin material were observed, but no amyloid was detected and no enhancement in thioflavin-T fluorescence was observed (Figure-2C). Thus EGCG is still a very effective inhibitor if added at the midpoint of the lag phase. We next examined a sample 17 hours after initiation of amyloid formation, but prior to addition of EGCG. This is near the end of the lag phase. Thin species are present (Figure-2D). EGCG was added and an aliquot was removed 33 hours later (50 hours total after amyloid formation was initiated). Thin material was observed, together with some short thicker structures and some amorphous material (Figure-2E, Supporting Information). No amyloid was observed by TEM and no enhancement in thioflavin-T fluorescence was detected, showing that EGCG is still acting as an inhibitor. Finally, we examined the consequences of adding the compound in the middle of the growth phase (blue curve in Figure-2). A decay of the thioflavin-T fluorescence is observed over the course of several hours followed by a slower decay to a final low level

plateau value. The final value is higher than the initial value measured before the start of amyloid formation. This suggests that EGCG induced remodeling is not the reverse of amyloid formation. The TEM image recorded before EGCG was added reveals arrays of amyloid fibers (Figure-2F). Another TEM was recorded 27 hours after the addition of EGCG, (50 hours total after amyloid formation was initiated), and shows that EGCG has remodeled the fibers, leading to amorphous material and some small spherical species (Figure-2G). Similar observations have been reported when EGCG is added after amyloid formation is complete (20). Remodeling of fully formed amyloid fibers follows a time course similar to what we observed here; namely an initial decay on the order of a few hours followed by a slow decay. The simplest explanation for the kinetic curve and the TEM images observed after EGCG is added in the middle of the growth phase is that the compound remodels the amyloid fibers which have formed at this stage and prevents any pre-fibril intermediates from forming fibers. The remodeling process is considered in more detail in the next subsection.

EGCG is a very potent inhibitor of amyloid formation; hence we examined the effects of adding a substoichiometric amount at different time points. We reasoned that any differences would be easier to detect under these conditions. EGCG is still an effective inhibitor when added at a ratio of EGCG to IAPP of 1 to 2 and is also effective if added after the initiation of amyloid formation, although some differential effects are observed depending upon when it is added (Supporting Information). These experiments show that EGCG is an effective inhibitor of IAPP amyloid formation no matter when it is added and implies that it interacts with a range of species populated during the lag phase.

Remodeling of IAPP amyloid by EGCG is not the reverse of amyloid formation

The data displayed in Figure-2 promoted us to examine the remodeling process in more detail. EGCG has been shown to remodel amyloid fibers formed by a range of polypeptides including IAPP (20–22). The observation that the final thioflavin-T intensity after the addition of EGCG does not reduce to the zero intensity baseline argues that EGCG induced remodeling is not the reverse of amyloid formation since monomeric IAPP does not induce thioflavin-T fluorescence. The experiments reported in Figure-2 and our earlier work were conducted using a 1:1 ratio of EGCG to IAPP (20). We examined the consequences of altering the ratio of EGCG to IAPP in order to test if the failure of the thioflavin-T fluorescence to completely decay was due to insufficient amounts of EGCG. This does not appear to be the case since the final thioflavin-T fluorescence reaches a limiting, non-zero value when excess EGCG is added. Figure-3 displays thioflavin-T remodeling curves for EGCG:IAPP ratios ranging from 0.5:1 to 5:1. The final thioflavin-T fluorescence intensity converges to the same value and does not return to the time=0 baseline (Figure-3B). Similar results are obtained if a 1:1 ratio of EGCG to IAPP is used to initiate the remodeling and more EGCG is then added when the reaction has reached a steady state (Supporting Information). TEM shows that the products of the remodeling reaction are not amyloid fibers and also differ from TEM images recorded of freshly dissolved IAPP. The thioflavin-T and TEM data argues against a remodeling mechanism in which IAPP fibers are in equilibrium with monomers and EGCG binds only to monomers and maintains them in a soluble form thereby shifting the equilibrium to the soluble state. In this scenario, the inhibitor would ultimately lead to complete lose of thioflavin-T signal and to TEM images which resemble those collected at time=0. Direct evidence against this mode of action is provided by studies which monitor the amount of soluble peptide present after EGCG is added to IAPP amyloid fibers. EGCG was added to IAPP amyloid fibers and the amount of soluble peptide was measured by centrifuging the resulting material at 20,000 g for 30 minutes and using Bradford assays to monitor the amount of peptide in the supernatant. These conditions were chosen because they pellet IAPP amyloid fibers. Control experiments

show that less than 8% of the peptide remains in the soluble fraction after centrifugation of a sample of IAPP amyloid in the absence of EGCG (Supporting Information). A second control experiment shows that addition of EGCG to freshly dissolved soluble IAPP at the start of an amyloid formation reaction maintains the peptide in solution. For this control experiment, EGCG was added to a sample of freshly dissolved IAPP and the solution was incubated for 50 hours. This time was chosen because it is much longer than the time required to form amyloid. After the centrifugation, more than 90% of the peptide was in the soluble fraction. Very different results are obtained if EGCG is added to preformed fibers. Close to 95% of the IAPP remained in the insoluble fraction after EGCG induced remodeling. For this experiment, a 16 μM sample of IAPP was incubated for 50 hours, a time for which fiber formation is complete, and EGCG was then added. The solution was incubated for another 45 hours and the amount of soluble protein was measured. The solubility measurements, TEM and thioflavin-T experiments show that EGCG induced remodeling of IAPP amyloid fibers leads to insoluble non-fibrillar material which retains a modest ability to bind thioflavin-T.

We next examined the ability of the material produced by the EGCG induced remodeling to seed amyloid formation by initially monomeric IAPP. Seeding experiments involve the addition of aggregated material to a solution of monomers. Seeds derived from amyloid fibers promote rapid amyloid formation by their own monomers and lead to a bypass of the lag phase. Seeding studies provide a convenient, albeit indirect, probe of structure since seeding typically exhibits a high degree of structural specificity (63). The material generated by the EGCG induced remodeling demonstrates no capacity to seed amyloid formation by IAPP, arguing that the final product is not simply small fragments of amyloid fibers with exposed ends (Figure-4).

Interactions with aromatic residues are not required for the inhibition of IAPP amyloid, or for the remodeling of IAPP amyloid by EGCG

π-stacking of aromatic residues has been proposed to contribute to amyloid formation, although aromatic aromatic interactions are not required for amyloid formation by IAPP or Aβ (49, 64–67). Interactions between the aromatic side chains of Phe, Tyr or Trp and aromatic rings of amyloid inhibitors have also been proposed to play an important role in drug polypeptide interactions (10, 12). Wild type IAPP contains 3 aromatic residues; F15, F23 and the C-terminal amidated Tyrosine. Phe-15 and Tyr-37 are rigorously conserved in all known IAPP sequences while Phe-23 is strongly conserved. In order to test the potential role of aromatic interactions in the inhibition of IAPP amyloid formation by EGCG we examined the ability of the compound to inhibit amyloid formation by two variants of IAPP. We have previously shown that a triple mutant of IAPP, denoted 3XL-IAPP in which the three aromatic residues are replaced by Leucines forms amyloid, albeit at a reduced rate (49). We also examined a second variant, denoted F15L, F23L-IAPP, in which F15 and F23 were mutated to Leu but Y37 was not.

Thioflavin-T kinetic curves of 3XL-IAPP recorded in the presence and absence of EGCG are displayed in Figure-5. Also included in the figure are TEM images collected at the end of the experiments. The data clearly demonstrates that EGCG is an effective inhibitor of amyloid formation by 3XL-IAPP and thus shows that interactions with aromatic residues are not required. The ability of EGCG to remodel preformed 3XL-IAPP amyloid fibers was also tested by adding EGCG after formation of amyloid fibers (Figure-6). The presence of amyloid was confirmed by removing an aliquot of the reaction mixture prior to the addition of EGCG. The thioflavin-T fluorescence intensity exhibited a multiphase decay after addition of EGCG which is very similar to that reported for wild type IAPP (20). TEM images recorded at the end of the time course confirmed that EGCG efficiently remodeled 3XL-IAPP amyloid fibers.

We examined the behavior of the second aromatic mutant in which F15 and F23 were replaced by Leucine, F15L, F23L-IAPP (Supporting Information). This polypeptide forms amyloid more rapidly than the 3XL mutant. EGCG also inhibited amyloid formation by this polypeptide and remodeled pre-formed F15L, F23L-IAPP amyloid fibers.

Interactions with Cys-2, Cys-7 or with free amino groups are not required for the inhibition of IAPP amyloid formation by EGCG or for the remodeling of IAAP amyloid by EGCG

We next examined the role of protein amino groups and the C2 C7 disulfide in IAPP EGCG interactions. Reaction with free thiols of reduced Cys residues and Schiff-base formation with the N-terminal amino group or with the ε-amino group of lysine side chains have been proposed to play a role in the action of EGCG (26). We used a truncated acetylated variant of IAPP, $IAPP_{AC8\text{-}37}$ (Figure-1), which comprises residues 8 to 37 of human IAPP. This peptide lacks the disulfide and is devoid of amino groups. $IAPP_{AC8\text{-}37}$ forms amyloid on the same time scale as full length IAPP and the morphology of the amyloid deposits are the same as judged by TEM (50). Figure 7 displays thioflavin-T curves for $IAPP_{AC8\text{-}37}$ in the presence and absence of EGCG. No change in thioflavin-T fluorescence is observed over the entire time course when EGCG is present. In contrast, a typical amyloid kinetic progress curve is observed in its absence. TEM images collected 30 hours after the initiation of amyloid formation reveal a dense mat of fibers in the absence of EGCG, but none in its presence (Figure-7). We studied the ability of EGCG to remodel amyloid fibers formed by $IAPP_{AC8\text{-}37}$ (Figure-8). A sample of the polypeptide was incubated for 30 hours and EGCG was added. TEM images of a sample removed just before the addition of EGCG showed typical amyloid fibers. An initial decay of thioflavin-T fluorescence was observed over several hours after addition of EGCG, followed by a slower decay. The curve is very similar to that observed for the remodeling of wild type IAPP amyloid fibers. No fibers were detected in the TEM image collected at the end of the time course. This set of experiments demonstrates that neither free amino groups nor the disulfide are required for EGCG's inhibition of amyloid formation by IAPP or for its ability to remodel pre-formed IAPP amyloid fibers.

In order to confirm these results, we examined a second peptide fragment derived from full length IAPP. The acetylated 8–24 fragment, $IAPP_{AC8\text{-}24}$, lacks free amino groups. Note that it also lacks the C-terminal tyrosine and thus provides a second independent test of the potential role of EGCG tyrosine interactions. The fragment forms amyloid on a similar time scale as the other peptides (Supporting Information). Thioflavin-T assays and TEM analysis reveal that EGCG efficiently inhibits amyloid formation by this peptide and remodels pre-formed amyloid fibers (Supporting Information). Our analysis of $IAPP_{AC8\text{-}24}$ confirms that interactions with free amino groups, or the disulfide, or the tyrosine side chain are not required for the action of EGCG.

The gallate ester and the integrity of the tri-hydroxyl phenyl ring are important for the effectiveness of EGCG

We analyzed several EGCG derivates in order to help define the features of the compound which are critical for its anti-IAPP amyloid activity. EGCG has been shown to inhibit a range of amyloid forming polypeptides, but little is known about the relative importance of the different groups in the molecule. Our goal is not to conduct a detailed structure function relationship study, but to probe several key features.

EGCG can epimerize to (−)-Gallocatechin gallate (GCG, Figure-1), when subjected to prolonged heating (68). Thus we examined the ability of GCG to inhibit IAPP amyloid formation. The compound is very effective, although slightly less so than EGCG. At a 1:1 ratio, GCG lengthens the lag time a factor of 4 and reduces the final thioflavin-T

fluorescence by 85% (Figure-9). TEM images of a sample removed at the end of the kinetic experiments show that there are much shorter and less dense mats of fibers formed than are found with wild type IAPP alone.

We then examined the effect of removing the gallate ester. Removal of the gallate group to produce EGC leads to a compound which is still an inhibitor of IAPP amyloid formation, although it is noticeably less effective (Figure-9). Retention of the gallate ester, but removal of one of the tri-hydroxyl groups leads to ECG (Figure-1). This simple modification has a significant effect upon the ability to inhibit IAPP amyloid formation. ECG is still an inhibitor, lengthening the lag phase by a factor of 2, and reducing the final thioflavin-T fluorescence by 63%, but is much less effective than EGCG. The observation of significant effects upon removal of either the hydroxyl or the gallate group naturally leads to the question of the effect of removing both. This modification leads to Epi-Catechin. This compound is of historical interest, as is its isomer catechin, because they were apparently the first polyphenols shown to inhibit formation of β-sheet structure (51), although their effects on amyloid were not tested in the early studies. Epi-catechin is not a good inhibitor of IAPP amyloid formation (Figure-9) nor is its isomer Catechin (Supporting Information). This analysis highlights the importance of both the gallate ester and the tri-hydroxyl phenyl structure. Additional experiments were conducted in the presence of a five-fold excess of the inhibitors. Under these conditions, ECG abolishes amyloid formation by IAPP, while EGC still does not, but it is more effective at this concentration (Supporting Information).

We then test the ability of these compounds to remodel pre-formed IAPP amyloid. Their relative performance, as judged by the final thioflavin-T fluorescence, closely tracked their relative effect on *de novo* amyloid formation. TEM studies confirm that GCG, ECG and EGC all remodel amyloid fibers. Interestingly, the TEM images of samples remodeled by different inhibitors appear very similar although there are differences in the relative ability to bind thioflavin-T. The relative order of the compounds to remodel IAPP fibers is similar to their reported ability to remodel α-synuclein amyloid fibers, suggesting there could be a common mode of action (22).

It is interesting to compare the apparent rate of remodeling induced by EGCG when it is added in the middle of the growth phase (Figure-2) to that observed when it is added in the plateau region (Figure-4). The time required to reach the final thioflavin-T value after the addition of EGCG is shorter when the compound is added in the middle of the growth phase (Supporting Information). The difference might reflect differences in fiber structure at the two time points, although our methods have insufficient resolution to detect any. The different effects may also be due to the simple fact that fewer fibers are present at the midpoint of the growth phase and the ratio of EGCG to fiber materials is thus higher at this point.

CONCLUSIONS

The data reported here clearly demonstrates that EGCG inhibits amyloid formation by IAPP when added to the lag phase and this suggests that it is able to bind to intermediates as well as to monomers and mature fibers. Interactions with aromatic residues, or the disulfide, or protein amino groups, or the tyrosine sidechain are not required for effective inhibition by EGCG. By process of elimination, it appears that EGCG interacts with IAPP by hydrogen bonding to the peptide backbone and by relatively non-specific, presumably hydrophobic interactions with sidechains. These observations are consistent with previous proposals that EGCG interacts, at least in part, with a range of sidechains (16, 24, 69). This mode of binding is fairly non-specific, which may help to explain why EGCG is so effective at inhibiting a wide range of natively unfolded polypeptides (16–23).

Our analysis of the EGCG derivatives shows that the isomer GCG is an effective inhibitor. Removal of the gallate ester has major effects, but the resulting compound still has some ability to inhibit amyloid. The removal of one of the hydroxyls from the tri-hydroxyl phenol ring also has a large effect. Removal of both the gallate ester and the hydroxyl abolishes the ability to inhibit IAPP amyloid formation under our conditions. Thus the most effective inhibitors among the compounds studied here contain two tri-hydroxyl phenyl rings. The presence of tri-hydroxyl substitutions has also been reported to be important for the ability of polyphenolic compounds to disaggregate α-synuclein oligomers (70).

The time dependent thioflavin-T studies, solubility experiments and TEM images conclusively show that EGCG induced remodeling is not the reverse of amyloid formation. The solubility studies and thioflavin-T data argue against a mechanism by which EGCG binds to soluble small oligomers and monomers and induces remodeling by shifting the equilibrium to a pool of EGCG stabilized soluble peptide. However, the data can not eliminate the possibility that EGCG remodels IAPP amyloid fibers by binding to soluble IAPP and then sequestering it in non-amyloid aggregates. Thus the exact mechanism of the EGCG induced remolding of IAPP amyloid is an open question and will be the subject of further studies.

Supplementary Material

Refer to Web version on PubMed Central for supplementary material.

Acknowledgments

We thank Ms. Ling-Hsien Tu for providing F15L, F23L mutants of IAPP and Dr. Andiesh Abedini and Mr. Harris Noor for helpful discussions.

+ Grant Sponsor NIH GM078114 to DPR

Abbreviations

CD	Circular Dichroism
ECG	(−)-Epicatechin gallate (−)-*cis*-2-(3,4-Dihydroxyphenyl)-3,4-dihydro-1(2H)-benzopyran-3,5,7-triol 3-gallate
EGC	(−)-Epigallocatechin, (−)-*cis*-2-(3,4,5-Trihydroxyphenyl)-3,4-dihydro-1(2H)-benzopyran-3,5,7-triol
EGCG	(−)-Epigallocatechin 3-gallate, (2*R*,3*R*)-5,7-dihydroxy-2-(3,4,5-trihydroxyphenyl)-3,4-dihydro-2*H*-1-benzopyran-3-yl 3,4,5-trihydroxybenzoate
Fmoc	9-fluorenylmethoxycarbonyl
GCG	(−)-Gallocatechin gallate, (2*S*,3*R*)-2-(3,4,5- Trihydroxyphenyl)-3,4-dihydro-1(2H)-benzopyran- 3,5,7- triol 3-(3,4,5-trihydroxybenzoate)
IAPP	human islet amyloid polypeptide
3XL-IAPP	the F15L/F23L/Y37L triple mutant of human IAPP
F15L	F23L-IAPP, the F15L/F23L double mutant of human IAPP
$IAPP_{Ac8\text{-}37}$	residues 8–37 of human IAPP with an amidated C terminus and an acetylated N terminus

$IAPP_{Ac8-24}$	residues 8–24 of human IAPP with an amidated C terminus and an acetylated N terminus
MALDI-TOF MS	matrix assisted laser desorption ionization-time of flight mass spectrometry
PAL-PEG	5-(4'-Fmoc-aminomethyl-3',5-dimethoxyphenyl) valeric acid
t_{50}	the time required to achieve 50% of the final thioflavin-T intensity in a kinetic experiment
TEM	transmission electron microscopy
TFA	trifluoroacetic acid.

References

1. Sipe JD. Amyloidosis. Critical Reviews in Clinical Laboratory Sciences. 1994; 31:325–354. [PubMed: 7888076]
2. Selkoe DJ. Cell biology of protein misfolding: The examples of Alzheimer's and Parkinson's diseases. Nat. Cell Biol. 2004; 6:1054–1061. [PubMed: 15516999]
3. Chiti F, Dobson CM. Protein misfolding, functional amyloid, and human disease. Annu. Rev. Biochem. 2006; 75:333–366. [PubMed: 16756495]
4. Yan LM, Tatarek-Nossol M, Velkova A, Kazantzis A, Kapurniotu A. Design of a mimic of nonamyloidogenic and bioactive human islet amyloid polypeptide (IAPP) as nanomolar affinity inhibitor of IAPP cytotoxic fibrillogenesis. Proc. Natl. Acad. SciU.SA. 2006; 103:2046–2051.
5. Feng BY, Toyama BH, Wille H, Colby DW, Collins SR, May BCH, Prusiner SB, Weissman J, Shoichet BK. Small-molecule aggregates inhibit amyloid polymerization. Nat. Chem. Biol. 2008; 4:197–199. [PubMed: 18223646]
6. Blazer LL, Neubig RR. Small molecule protein-protein interaction inhibitors as CNS therapeutic agents: current progress and future hurdles. Neuropsychopharmacol. 2009; 34:126–141.
7. Takahashi T, Mihara H. Peptide and protein mimetics inhibiting amyloid beta-peptide aggregation. Accounts Chem. Res. 2008; 41:1309–1318.
8. Abedini A, Meng FL, Raleigh DP. A single-point mutation converts the highly amyloidogenic human islet amyloid polypeptide into a potent fibrillization inhibitor. J. Am. Chem. Soc. 2007; 129:11300–11301. [PubMed: 17722920]
9. Scrocchi LA, Chen Y, Wang F, Han K, Ha K, Wu L, Fraser PE. Inhibitors of islet amyloid polypeptide fibrillogenesis, and the treatment of type-2 diabetes. Lett. Pept. Sci. 2003; 10:545–551.
10. Porat Y, Mazor Y, Efrat S, Gazit E. Inhibition of islet amyloid polypeptide fibril formation: A potential role for heteroaromatic interactions. Biochemistry. 2004; 43:14454–14462. [PubMed: 15533050]
11. Mishra R, Bulic B, Sellin D, Jha S, Waldmann H, Winter R. Small-molecule inhibitors of islet amyloid polypeptide fibril formation. Angew. Chem. Int. Edit. 2008; 47:4679–4682.
12. Porat Y, Abramowitz A, Gazit E. Inhibition of amyloid fibril formation by polyphenols: Structural similarity and aromatic interactions as a common inhibition mechanism. Chem. Biol. Drug Des. 2006; 67:27–37. [PubMed: 16492146]
13. Meng FL, Abedini A, Raleigh DP. Combination of kinetically selected inhibitors in trans leads to highly effective inhibition of amyloid formation. J. Am. Chem. Soc. 2010; 132:14340–14342. [PubMed: 20873820]
14. Bieschke J, Herbst M, Wiglenda T, Friedrich RP, Boeddrich A, Schiele F, Kleckers D, del Amo JML, Gruning BA, Wang QW, Schmidt MR, Lurz R, Anwyl R, Schnoegl S, Fandrich M, Frank RF, Reif B, Gunther S, Walsh DM, Wanker EE. Small-molecule conversion of toxic oligomers to nontoxic beta-sheet-rich amyloid fibrils. Nat. Chem. Biol. 2012; 8:93–101. [PubMed: 22101602]

15. Noor H, Cao P, Raleigh DP. Morin hydrate inhibits amyloid formation by islet amyloid polypeptide and disaggregates amyloid fibers. Protein Sci. 2012; 21:373–382. [PubMed: 22238175]

16. Ehrnhoefer DE, Bieschke J, Boeddrich A, Herbst M, Masino L, Lurz R, Engemann S, Pastore A, Wanker EE. EGCG redirects amyloidogenic polypeptides into unstructured, off-pathway oligomers. Nat. Struct. Mol. Biol. 2008; 15:558–566. [PubMed: 18511942]

17. Rambold AS, Miesbauer M, Olschewski D, Seidel R, Riemer C, Smale L, Brumm L, Levy M, Gazit E, Oesterhelt D, Baier M, Becker CFW, Engelhard M, Winklhofer KF, Tatzelt J. Green tea extracts interfere with the stress-protective activity of PrP(C) and the formation of PrP(Sc). J. Neurochem. 2008; 107:218–229. [PubMed: 18691383]

18. Masuda M, Suzuki N, Taniguchi S, Oikawa T, Nonaka T, Iwatsubo T, Hisanaga S, Goedert M, Hasegawa M. Small molecule inhibitors of alpha-synuclein filament assembly. Biochemistry. 2006; 45:6085–6094. [PubMed: 16681381]

19. Ehrnhoefer DE, Duennwald M, Markovic P, Wacker JL, Engemann S, Roark M, Legleiter J, Marsh JL, Thompson LM, Lindquist S, Muchowski PJ, Wanker EE. Green tea (−)-epigallocatechin-gallate modulates early events in Huntingtin misfolding and reduces toxicity in Huntington's disease models. Hum. Mol. Genet. 2006; 15:2743–2751. [PubMed: 16893904]

20. Meng FL, Abedini A, Plesner A, Verchere CB, Raleigh DP. The Flavanol (−)-Epigallocatechin 3-Gallate inhibits amyloid formation by islet amyloid polypeptide, disaggregates amyloid fibrils, and protects cultured cells against IAPP-induced toxicity. Biochemistry. 2010; 49:8127–8133. [PubMed: 20707388]

21. Chandrashekaran IR, Adda CG, MacRaild CA, Anders RF, Norton RS. EGCG disaggregates amyloid-like fibrils formed by Plasmodium falciparum merozoite surface protein 2. Arch. Biochem. Biophys. 2011; 513:153–157. [PubMed: 21784057]

22. Bieschke J, Russ J, Friedrich RP, Ehrnhoefer DE, Wobst H, Neugebauer K, Wanker EE. EGCG remodels mature alpha-synuclein and amyloid-beta fibrils and reduces cellular toxicity. Proc. Natl. Acad. Sci. U.S.A. 2010; 107:7710–7715. [PubMed: 20385841]

23. Hauber I, Hohenberg H, Holstermann B, Hunstein W, Hauber J. The main green tea polyphenol epigallocatechin-3-gallate counteracts semen-mediated enhancement of HIV infection. Proc. Natl. Acad. Sci. U.S.A. 2009; 106:9033–9038. [PubMed: 19451623]

24. Hudson SA, Ecroyd H, Dehle FC, Musgrave IF, Carver JA. (−)-Epigallocatechin-3-Gallate (EGCG) maintains kappa-casein in its pre-fibrillar state without redirecting its aggregation pathway. J. Mol. Biol. 2009; 392:689–700. [PubMed: 19616561]

25. Masuda M, Hasegawa M, Nonaka T, Oikawa T, Yonetani M, Yamaguchi Y, Kato K, Hisanaga S, Goedert M. Inhibition of alpha-synuclein fibril assembly by small molecules: Analysis using epitope-specific antibodies. Febs. Lett. 2009; 583:787–791. [PubMed: 19183551]

26. Qian XH, Cao D, Zhang YJ, Zhang HH, Zhong LW. Systematic characterization of the covalent interactions between (−)-epigallocatechin gallate and peptides under physiological conditions by mass spectrometry. Rapid Commun. Mass Sp. 2009; 23:1147–1157.

27. Zorilla R, Liang L, Remondetto G, Subirade M. Interaction of epigallocatechin-3-gallate with beta-lactoglobulin: molecular characterization and biological implication. Dairy Sci. Technol. 2011; 91:629–644.

28. Mori T, Ishii T, Akagawa M, Nakamura Y, Nakayama T. Covalent binding of tea catechins to protein thiols: the relationship between stability and electrophilic reactivity. Biosci. Biotech. Bioch. 2010; 74:2451–2456.

29. Westermark P, Wernstedt C, Wilander E, Hayden DW, Obrien TD, Johnson KH. Amyloid fibrils in human insulinoma and islets of langerhans of the diabetic cat are derived from a neuropeptide-like protein also present in normal islet cells. Proc. Natl. Acad. Sci. U.S.A. 1987; 84:3881–3885. [PubMed: 3035556]

30. Cooper GJS, Willis AC, Clark A, Turner RC, Sim RB, Reid KBM. Purification and characterization of a peptide from amyloid-rich pancreases of type-2 diabetic-patients. Proc. Natl. Acad. Sci. U.S.A. 1987; 84:8628–8632. [PubMed: 3317417]

31. Cooper GJS. Amylin compared with calcitonin-gene-related peptide - structure, biology, and relevance to metabolic disease. Endocr. Rev. 1994; 15:163–201. [PubMed: 8026387]

32. Hay DL, Christopoulos G, Christopoulos A, Sexton PM. Amylin receptors: molecular composition and pharmacology. Biochem. Soc. Trans. 2004; 32:865–867. [PubMed: 15494035]
33. Nishi M, Sanke T, Nagamatsu S, Bell GI, Steiner DF. Islet amyloid polypeptide - a new beta-cell secretory product related to islet amyloid deposits. J. Biol. Chem. 1990; 265:4173–4176. [PubMed: 2407732]
34. Hutton JC. The insulin secretory granule. Diabetologia. 1989; 32:271–281. [PubMed: 2526768]
35. Kahn SE, Andrikopoulos S, Verchere CB. Islet amyloid: A long-recognized but underappreciated pathological feature of type 2 diabetes. Diabetes. 1999; 48:241–253. [PubMed: 10334297]
36. Clark A, Cooper GJS, Morris JF, Lewis CE, Willis AC, Reid KBM, Turner RC. Islet amyloid formed from diabetes-associated peptide may be pathogenic in type-2 diabetes. Lancet. 1987; 2:231–234. [PubMed: 2441214]
37. Hull RL, Westermark GT, Westermark P, Kahn SE. Islet amyloid: A critical entity in the pathogenesis of type 2 diabetes. J. Clin. Endocr. Metab. 2004; 89:3629–3643. [PubMed: 15292279]
38. Marzban L, Park K, Verchere CB. Islet amyloid polypeptide and type 2 diabetes. Exp. Gerontol. 2003; 38:347–351. [PubMed: 12670620]
39. Lorenzo A, Razzaboni B, Weir GC, Yankner BA. Pancreatic-islet cell toxicity of amylin associated with type-2 diabetes-mellitus. Nature. 1994; 368:756–760. [PubMed: 8152488]
40. Clark A, Wells CA, Buley ID, Cruickshank JK, Vanhegan RI, Matthews DR, Cooper GJS, Holman RR, Turner RC. Islet amyloid, increased alpha-cells, reduced beta-cells and exocrine fibrosis - quantitative changes in the pancreas in type-2 diabetes. Diabetes Res. Clin. Ex. 1988; 9:151–159.
41. Butler AE, Janson J, Bonner-Weir S, Ritzel R, Rizza RA, Butler PC. beta-cell deficit and increased beta-cell apoptosis in humans with type 2 diabetes. Diabetes. 2003; 52:102–110. [PubMed: 12502499]
42. Hayden MR, Karuparthi PR, Manrique CM, Lastra G, Habibi J, Sowers JR. Longitudinal ultrastructure study of islet amyloid in the HIP rat model of type 2 diabetes mellitus. Exp. Biol. Med. 2007; 232:772–779.
43. Westermark GT, Westermark P, Berne C, Korsgren O, Transpla NNCI. Widespread amyloid deposition in transplanted human pancreatic islets. New Engl. J. Med. 2008; 359:977–979. [PubMed: 18753660]
44. Kirkitadze MD, Bitan G, Teplow DB. Paradigm shifts in Alzheimer's disease and other neuro degenerative disorders: The emerging role of oligomeric assemblies. J. Neurosci. Res. 2002; 69:567–577. [PubMed: 12210822]
45. Potter KJ, Abedini A, Marek P, Klimek AM, Butterworth S, Driscoll M, Baker R, Nilsson MR, Warnock GL, Oberholzer J, Bertera S, Trucco M, Korbutt GS, Fraser PE, Raleigh DP, Verchere CB. Islet amyloid deposition limits the viability of human islet grafts but not porcine islet grafts. Proc. Natl. Acad. Sci. U.S.A. 2010; 107:4305–4310. [PubMed: 20160085]
46. Abedini A, Raleigh DP. Incorporation of pseudoproline derivatives allows the facile synthesis of human IAPP, a highly amyloidogenic and aggregation-prone polypeptide. Org. Lett. 2005; 7:693–696. [PubMed: 15704927]
47. Abedini A, Singh G, Raleigh DP. Recovery and purification of highly aggregation-prone disulfide-containing peptides: Application to islet amyloid polypeptide. Anal. Biochem. 2006; 351:181–186. [PubMed: 16406209]
48. Nilsson MR, Driscoll M, Raleigh DP. Low levels of asparagine deamidation can have a dramatic effect on aggregation of amyloidogenic peptides: Implications for the study of amyloid formation. Protein Sci. 2002; 11:342–349. [PubMed: 11790844]
49. Marek P, Abedini A, Song BB, Kanungo M, Johnson ME, Gupta R, Zaman W, Wong SS, Raleigh DP. Aromatic interactions are not required for amyloid fibril formation by islet amyloid polypeptide but do influence the rate of fibril formation and fibril morphology. Biochemistry. 2007; 46:3255–3261. [PubMed: 17311418]
50. Abedini A, Raleigh DP. The role of His-18 in amyloid formation by human islet amyloid polypeptide. Biochemistry. 2005; 44:16284–16291. [PubMed: 16331989]
51. Tilstra LF, Maeda H, Mattice WL. Interaction of (+)-catechin with the edge of the beta-sheet formed by poly-(s-carboxymethyl-L-cysteine). J. Chem. Soc. Perk. T. 1988; 2:1613–1616.

52. Levine H. Thioflavine-T interaction with amyloid beta-sheet structures. Amyloid. 1995; 2:1–6.
53. Marek P, Mukherjee S, Zanni MT, Raleigh DP. Residue-specific, real-time characterization of lag-phase species and fibril growth during amyloid formation: A combined fluorescence and IR study of *p*-cyanophenylalanine analogs of islet amyloid polypeptide. J. Mol. Biol. 2010; 400:878–888. [PubMed: 20630475]
54. Meng FL, Marek P, Potter KJ, Verchere CB, Raleigh DP. Rifampicin does not prevent amyloid fibril formation by human islet amyloid polypeptide but does inhibit fibril thioflavin-T interactions: Implications for mechanistic studies beta-cell death. Biochemistry. 2008; 47:6016–6024. [PubMed: 18457428]
55. Hudson SA, Ecroyd H, Kee TW, Carver JA. The thioflavin T fluorescence assay for amyloid fibril detection can be biased by the presence of exogenous compounds. Febs. J. 2009; 276:5960–5972. [PubMed: 19754881]
56. Abedini A, Raleigh DP. A role for helical intermediates in amyloid formation by natively unfolded polypeptides? Phys. Biol. 2009; 6 015005.
57. Abedini A, Raleigh DP. A critical assessment of the role of helical intermediates in amyloid formation by natively unfolded proteins and polypeptides. Protein Eng. Des. Sel. 2009; 22:453–459. [PubMed: 19596696]
58. Williamson JA, Loria JP, Miranker AD. Helix stabilization precedes aqueous and bilayer-catalyzed fiber formation in islet amyloid polypeptide. J. Mol. Biol. 2009; 393:383–396. [PubMed: 19647750]
59. Wiltzius JJW, Sievers SA, Sawaya MR, Eisenberg D. Atomic structures of IAPP (amylin) fusions suggest a mechanism for fibrillation and the role of insulin in the process. Protein Sci. 2009; 18:1521–1530. [PubMed: 19475663]
60. Cao P, Meng F, Abedini A, Raleigh DP. The ability of rodent islet amyloid polypeptide to inhibit amyloid formation by human islet amyloid polypeptide has important implications for the mechanism of amyloid formation and the design of inhibitors. Biochemistry. 2010; 49:872–881. [PubMed: 20028124]
61. Williamson JA, Miranker AD. Direct detection of transient alpha-helical states in islet amyloid polypeptide. Protein Sci. 2007; 16:110–117. [PubMed: 17123962]
62. Dupuis NF, Wu C, Shea JE, Bowers MT. Human islet amyloid polypeptide monomers form ordered beta-hairpins: A possible direct amyloidogenic precursor. J. Am. Chem. Soc. 2009; 131:18283–18292. [PubMed: 19950949]
63. O'Nuallain B, Williams AD, Westermark P, Wetzel R. Seeding specificity in amyloid growth induced by heterologous fibrils. J. Biol. Chem. 2004; 279:17490–17499. [PubMed: 14752113]
64. Gazit E. A possible role for pi-stacking in the self-assembly of amyloid fibrils. Faseb. J. 2002; 16:77–83. [PubMed: 11772939]
65. Azriel R, Gazit E. Analysis of the structural and functional elements of the minimal active fragment of islet amyloid polypeptide (IAPP) - An experimental support for the key role of the phenylalanine residue in amyloid formation. J. Biol. Chem. 2001; 276:34156–34161. [PubMed: 11445568]
66. Tracz SM, Abedini A, Driscoll M, Raleigh DP. Role of aromatic interactions in amyloid formation by peptides derived from human amylin. Biochemistry. 2004; 43:15901–15908. [PubMed: 15595845]
67. Armstrong AH, Chen J, McKoy AF, Hecht MH. Mutations that replace aromatic side chains promote aggregation of the Alzheimer's A beta peptide. Biochemistry. 2011; 50:4058–4067. [PubMed: 21513285]
68. Chen ZY, Zhu QY, Tsang D, Huang Y. Degradation of green tea catechins in tea drinks. J. Agr. Food Chem. 2001; 49:477–482. [PubMed: 11170614]
69. Liu FF, Dong XY, He LZ, Middelberg APJ, Sun Y. Molecular insight into conformational transition of amyloid beta-peptide 42 inhibited by (−)-epigallocatechin-3-gallate probed by molecular simulations. J. Phys. Chem. B. 2011; 115:11879–11887. [PubMed: 21899367]
70. Caruana M, Hogen T, Levin J, Hillmer A, Giese A, Vassallo N. Inhibition and disaggregation of alpha-synuclein oligomers by natural polyphenolic compounds. Febs. Lett. 2011; 585:1113–1120. [PubMed: 21443877]

(A)

Human IAPP:

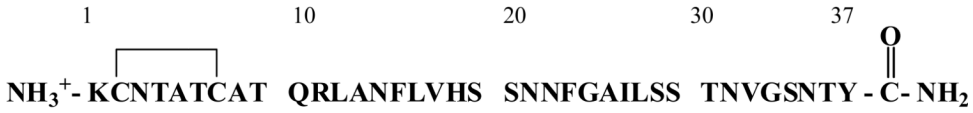

F15L, F23L IAPP:

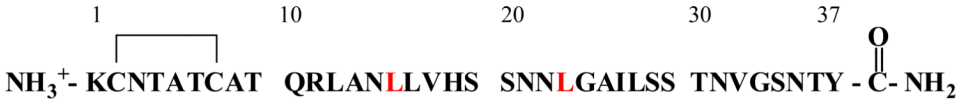

3XL-IAPP:

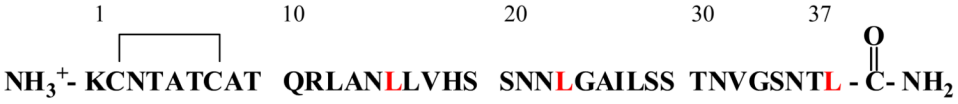

$IAPP_{Ac8-37}$

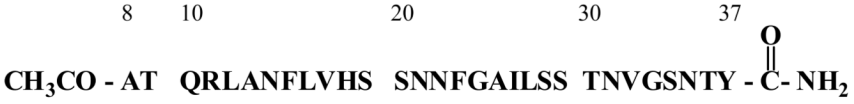

$IAPP_{Ac8-24}$

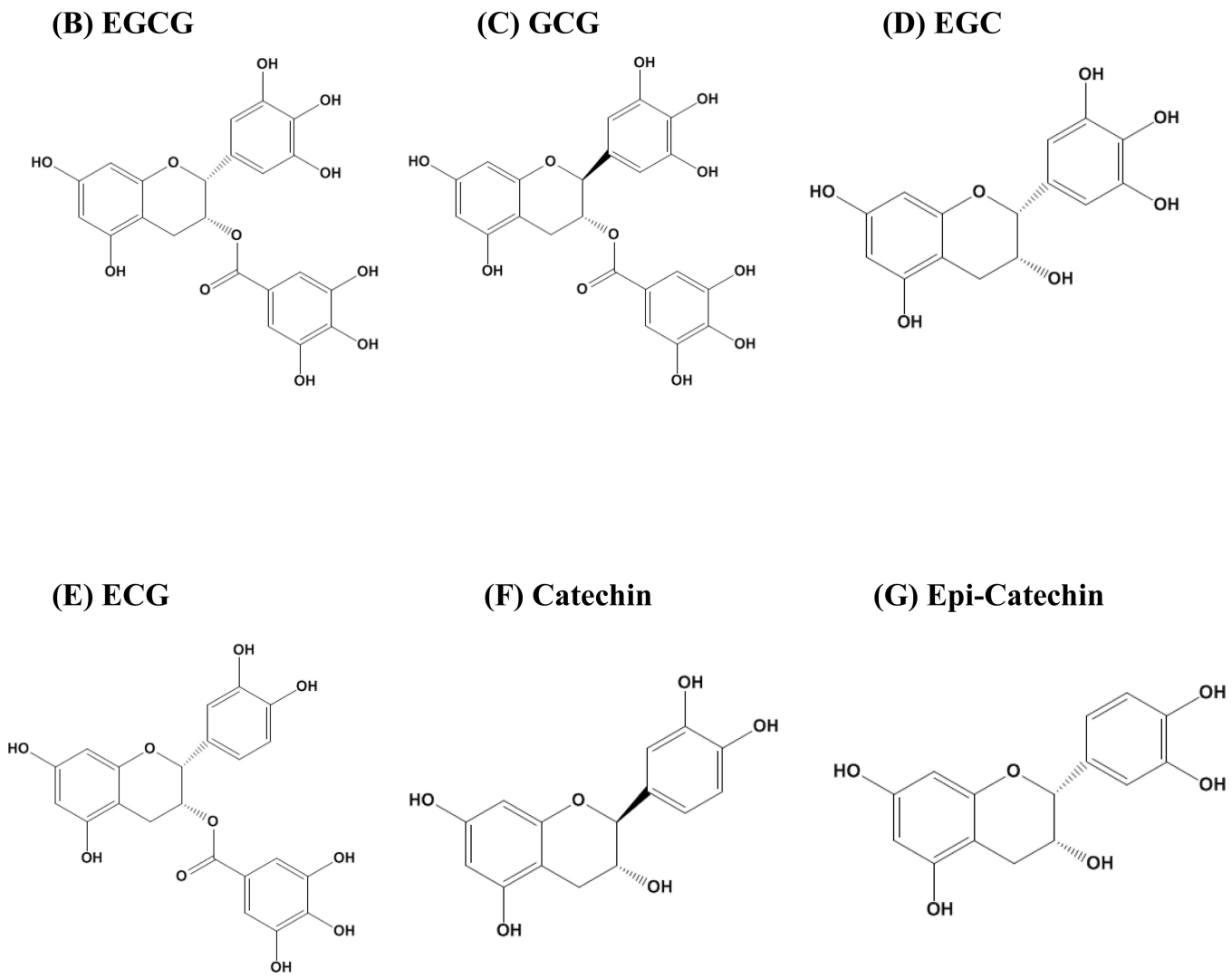

Figure 1.

(A) The primary sequence of human IAPP and the variants studied here. The wild type peptide contains a disulfide bridge between Cys-2 and Cys-7 and has an amidated C-terminus. (B) The structure of EGCG. (C) The structure of GCG. (D) The structure of EGC. (E) The structure of ECG. (F) The structure of Catechin. (G) The structure of Epi-Catechin.

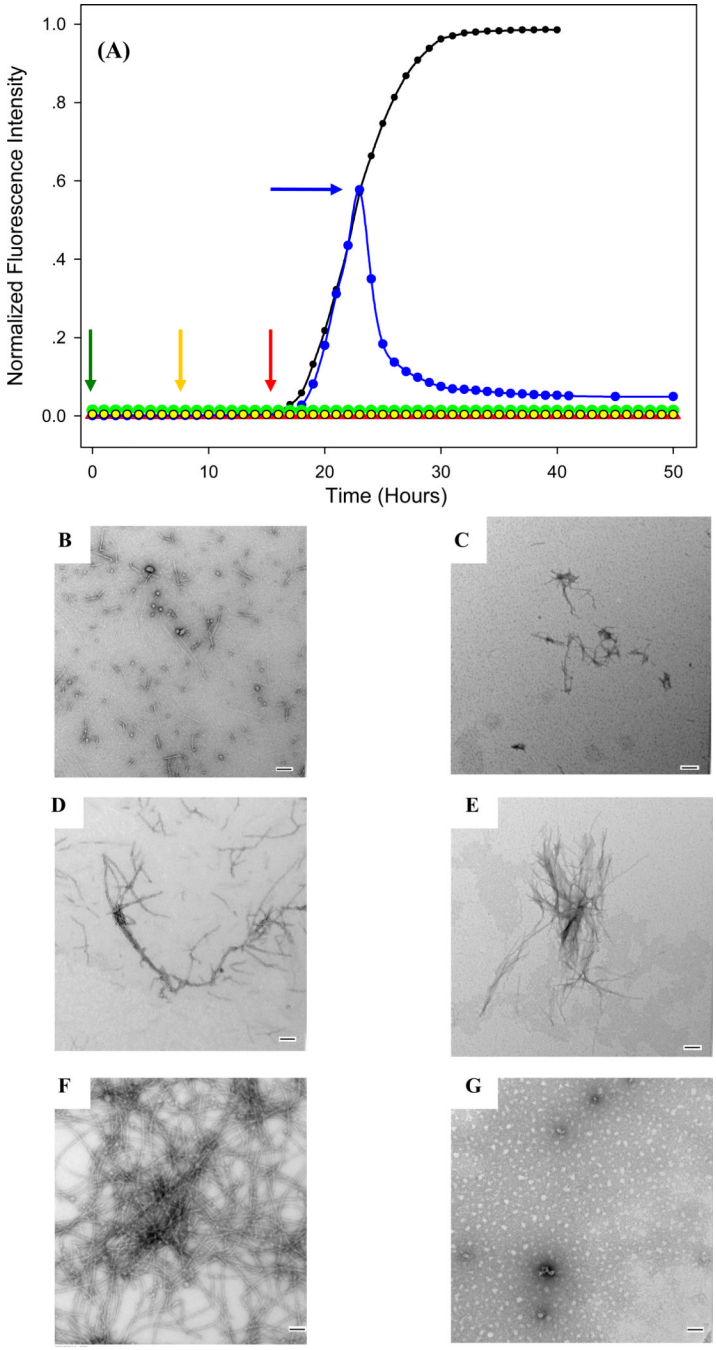

Figure 2.

The effect of adding an equal amount of EGCG at various time points during amyloid formation by IAPP. (A) Thioflavin-T monitored kinetic experiments are shown: Black, IAPP alone, no EGCG; Green, EGCG was added at time=0, time point indicated by green arrow; Yellow, EGCG was added in the lag phase, at the point indicted by the yellow arrow; Red, EGCG was added at the end of the lag phase, at the time point indicated by red arrow; Blue, EGCG was added midway through the growth phase, at the blue arrow. TEM images of samples recorded before and after the addition of EGCG. Samples were removed immediately before EGCG was added and analyzed by TEM. The solution was then allowed to sit for an addition time and aliquots were removed after a total incubation time of 50

hours, measured from the initiation of amyloid formation. (B) Wild type IAPP in the middle of the lag phase before the addition of EGCG (yellow arrow). (C) Wild type IAPP an additional 43 hours after adding EGCG. (D) Wild type IAPP at the end of the lag phase before the addition of EGCG (red arrow). (E) Wild type IAPP an additional 33 hours after adding EGCG. (F) Wild type IAPP in the growth phase before the addition of EGCG (blue arrow). (G) Wild type IAPP an additional 27 hours after adding EGCG. Scale bars are 100 nm. Experiments were conducted at 25°C, pH 7.4, 20 mM Tris-HCl, 32 micromolar thioflavin-T, 16 micromolar IAPP, EGCG when present was at 16 micromolar.

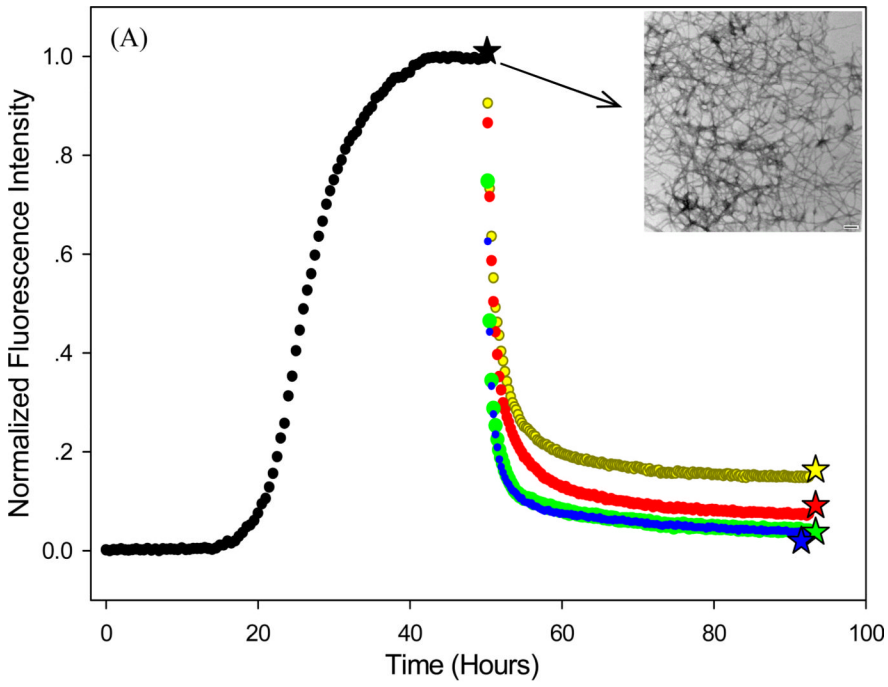

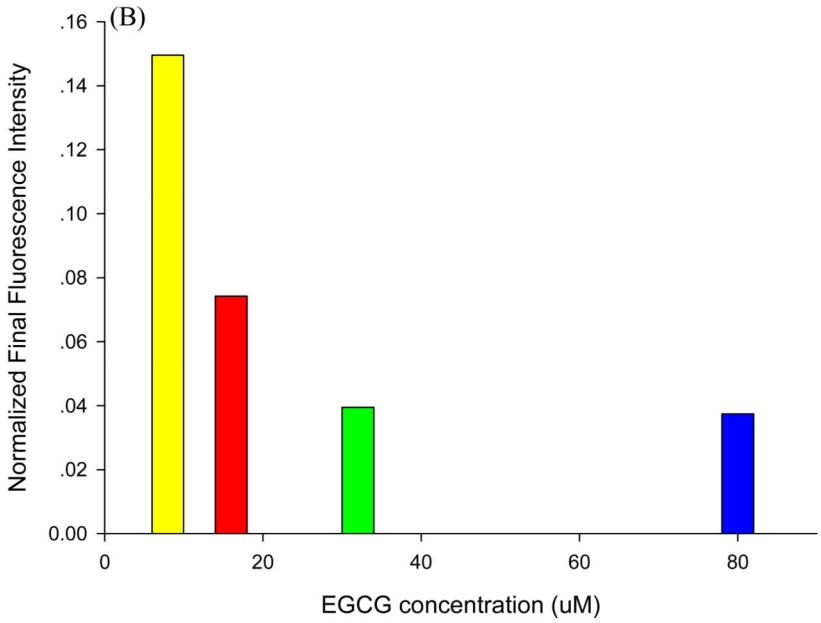

(C)

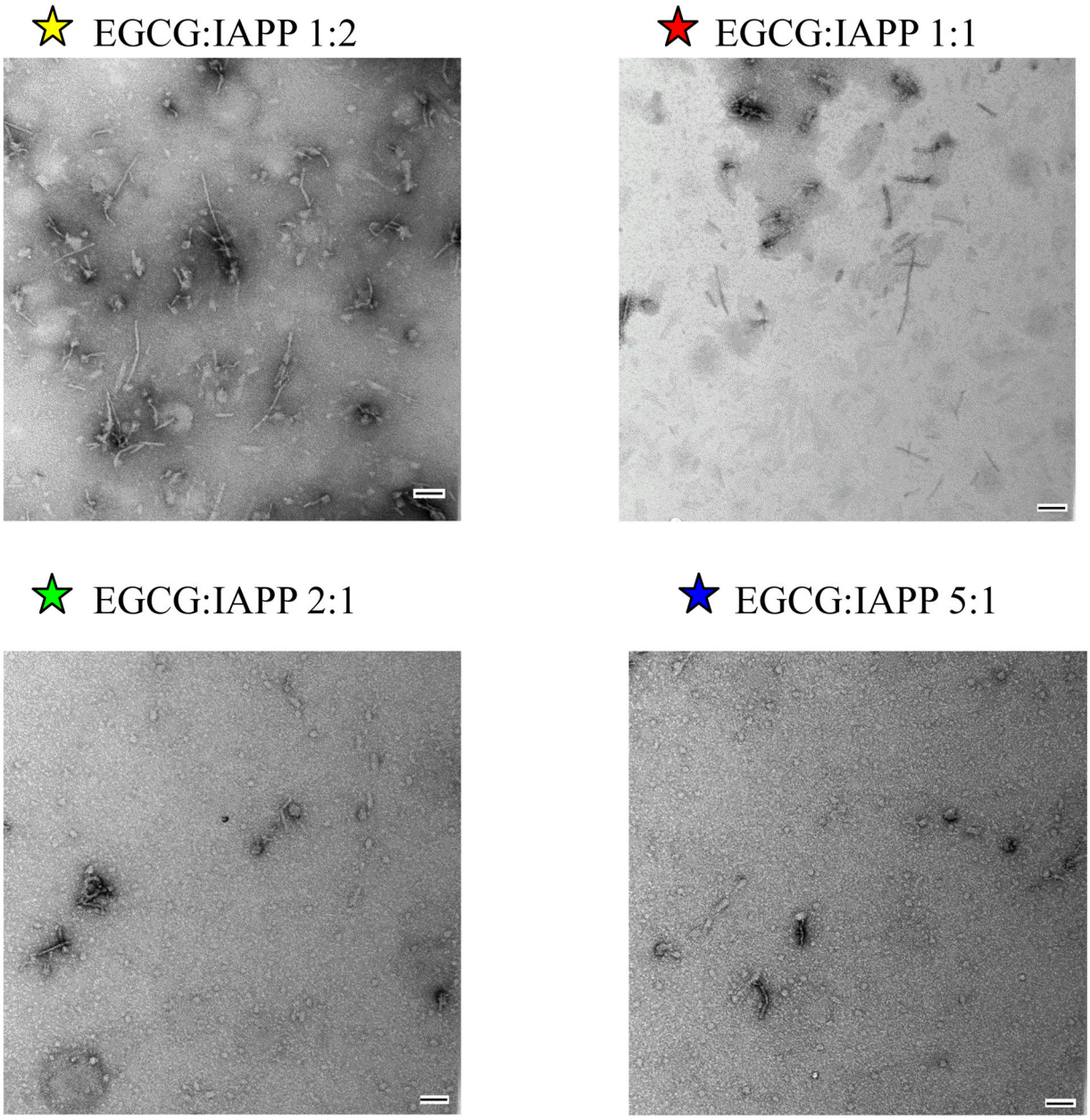

Figure 3.

Remodeling of IAPP amyloid fibers using different ratios of EGCG to IAPP. (A) Thioflavin-T kinetic curves. A 16 micromolar sample of human IAPP was allowed to form amyloid (black curve) and the presence of amyloid fibers was confirmed by TEM (insert). Various amounts of EGCG were added at the time point indicated by the black star (★). Yellow, 16 μM IAPP, 8 μM EGCG; Red, 16 μM IAPP, 16 μM EGCG; Green, 16 μM IAPP, 32 μM EGCG; Blue, 16 μM IAPP, 80 μM EGCG. (B) A bar graph of the final relative fluorescence intensity at the point indicated by the colored stars in panel-A. The same color coding is used. (C) TEM images of samples collected at the time points corresponding to

colored stars in panel-A. TEM images are labeled and color coded. Scale bars are 100 nm. Experiments were conducted at 25°C, pH 7.4, 20 mM Tris-HCl.

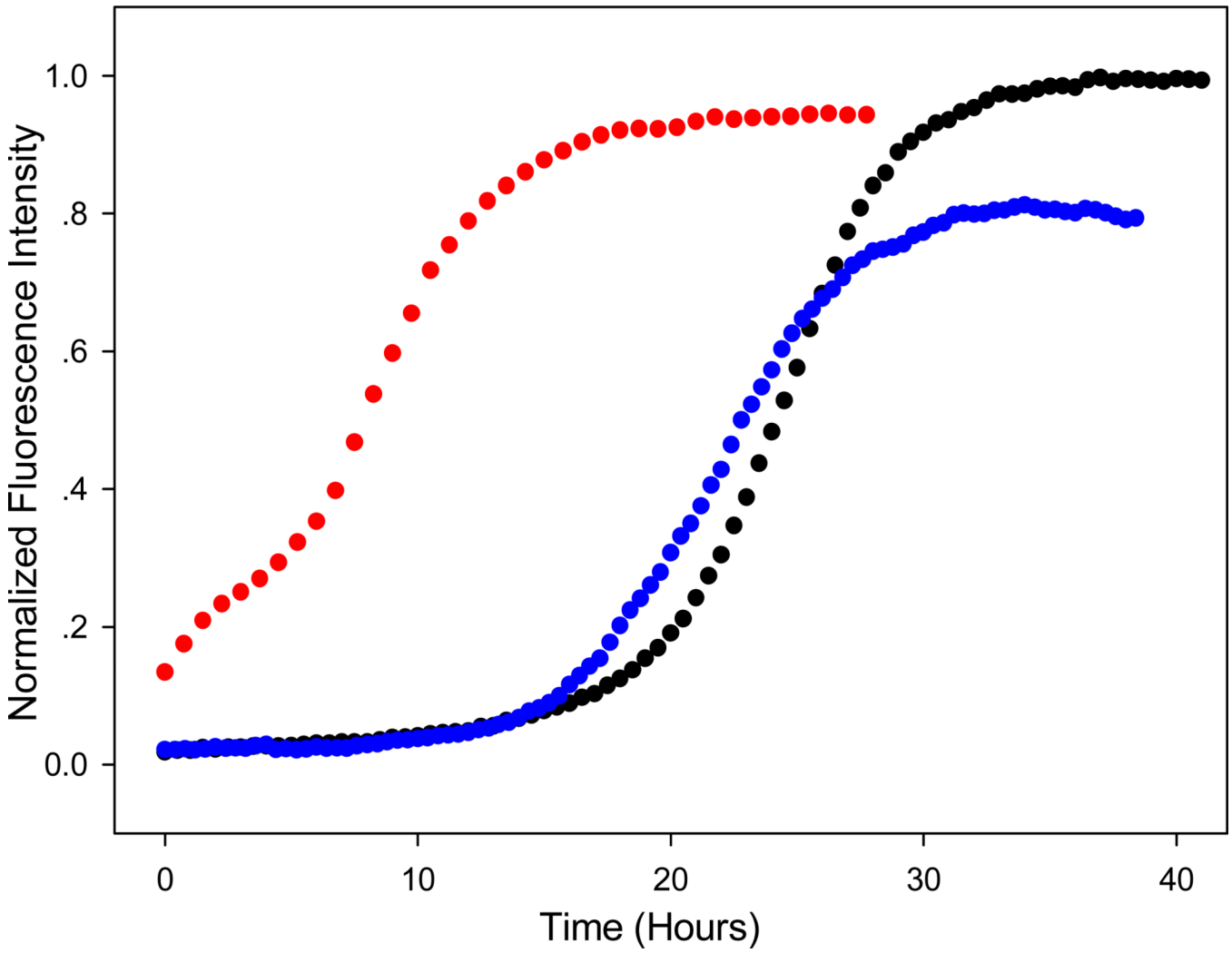

Figure 4.

The species which results from the remodeling of IAPP amyloid by EGCG does not seed amyloid formation by wild type IAPP. Thioflavin-T kinetic curves are shown. Black curve: unseeded human IAPP. Red curve: control experiment, IAPP seeded by IAPP amyloid fibers. Blue curve: IAPP seeded by EGCG induced remodeling material. Experiments were conducted at 25°C, pH 7.4, 20 mM Tris-HCl, 16 micromolar IAPP. Seeds, when present, were at 10% concentration in monomer units. The seeds for the remodeling material were obtained by adding 16 μM EGCG to 16 μM IAPP amyloid fibers and waiting for 45 hours. The initial intensity in the control experiment (seeding of IAPP by IAPP amyloid fibers) is not zero because the seed bind thioflavin-T.

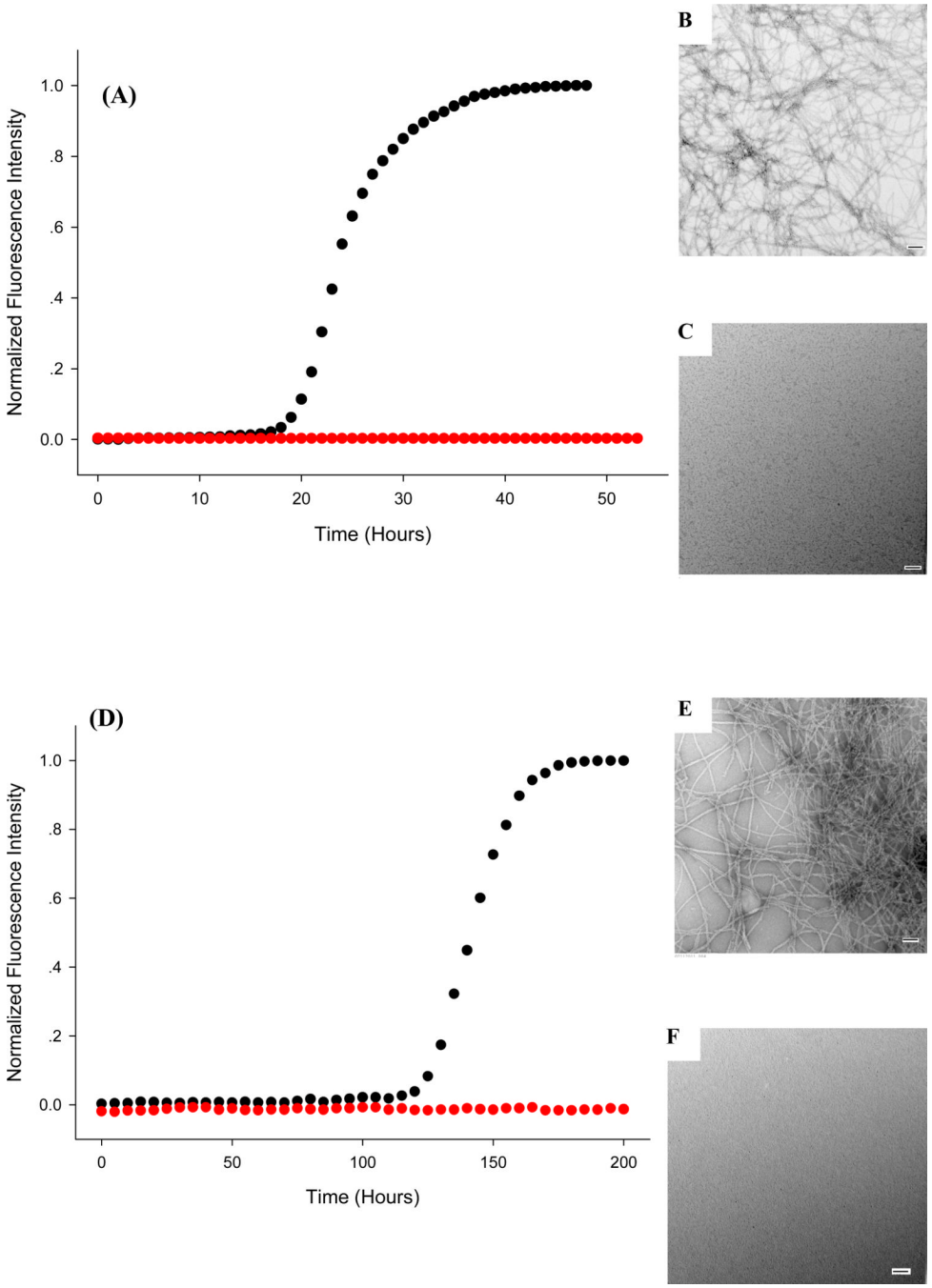

Figure 5.

Interactions with aromatic residues are not required for the inhibition of amyloid formation. (A) Control experiments with wild type IAPP. Thioflavin-T monitored kinetic experiments are shown in the presence (red) and absence of (black) EGCG. TEM images recorded of samples removed after 50 hours are displayed. (B) Wild type IAPP without EGCG. (C) Wild type IAPP with EGCG. (D) Inhibition of amyloid formation by the 3XL mutant of IAPP. Thioflavin-T monitored kinetic experiments are shown in the presence (red) and in the absence (black) of EGCG. TEM images recorded of samples removed after 200 hours are displayed. (E) 3XL-IAPP without EGCG. (F) 3XL-IAPP with EGCG. Scale bars are 100

nm. Experiments were conducted at 25°C, pH 7.4, 20 mM Tris-HCl, 32 micromolar thioflavin-T, 16 micromolar IAPP, EGCG when present was at 16 micromolar.

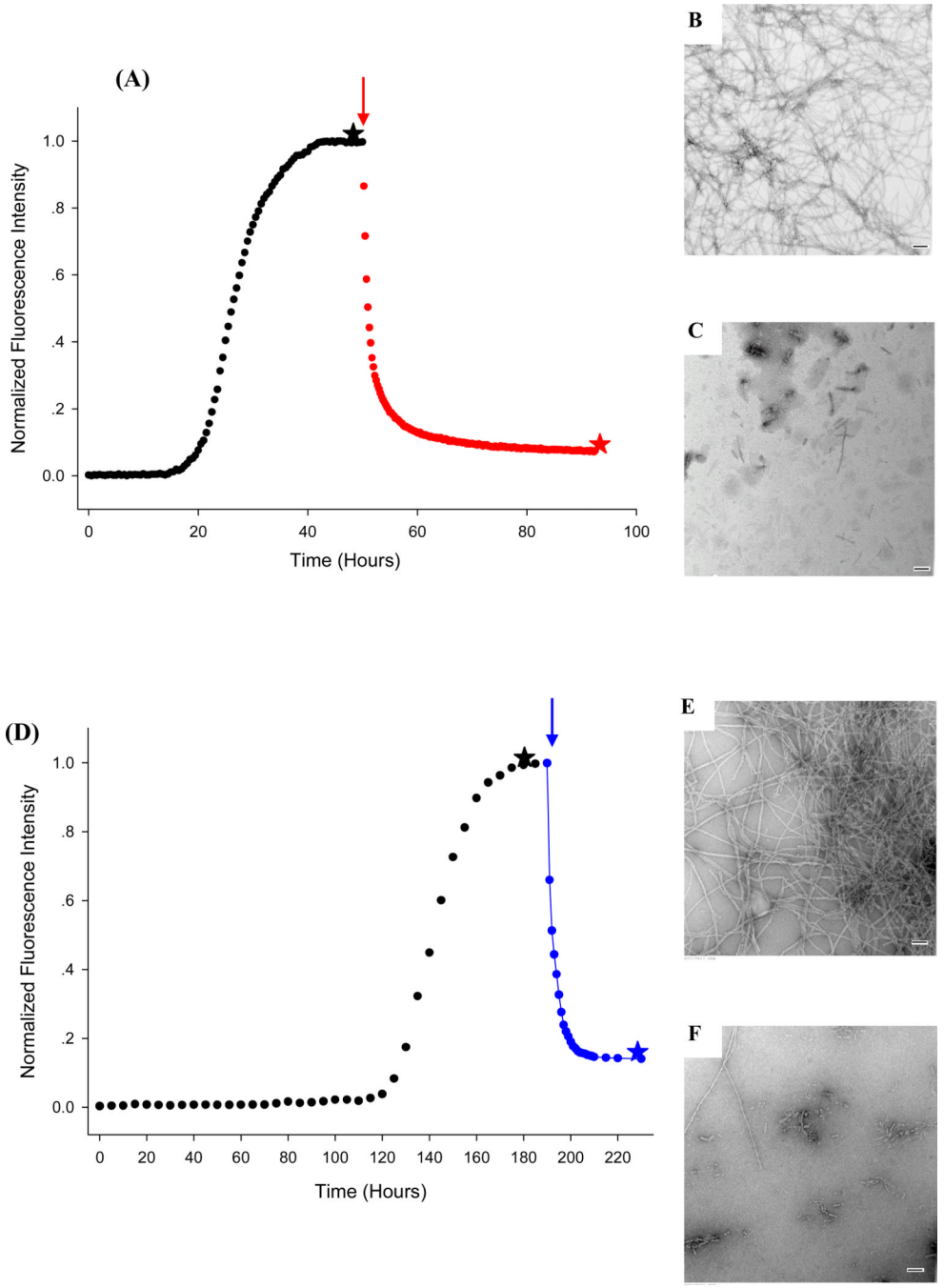

Figure 6.

Interactions with aromatic residues are not required for the effective remodeling of pre-formed IAPP amyloid fibers. Remodeling of wild type IAPP amyloid fibers by EGCG: (A) Thioflavin-T-monitored kinetic experiments: black, IAPP alone; red, EGCG added at the point indicated by the arrow. (B) TEM image of IAPP before the addition of EGCG, collected from a sample removed at the time point indicated by the black star. (C) TEM image collected after the addition of EGCG from a sample removed at the time point corresponding to the red star. Remodeling of 3XL-IAPP amyloid fibers by EGCG: (D) Thioflavin-T-monitored kinetic experiments: black, 3XL-IAPP alone; blue, EGCG added at the point indicated by the blue arrow. (E) TEM image of IAPP before the addition of EGCG,

collected from a sample removed at the time point indicated by the black star. (F) TEM image collected after the addition of EGCG from a sample removed at the time point corresponding to the blue star. Scale bars are 100 nm. Experiments were conducted at 25°C, pH 7.4, 20 mM Tris-HCl, 32 micromolar thioflavin-T, 16 micromolar IAPP, EGCG when present was at 16 micromolar. Note the different scale used for the X-axis in Panel-A and Panel-D.

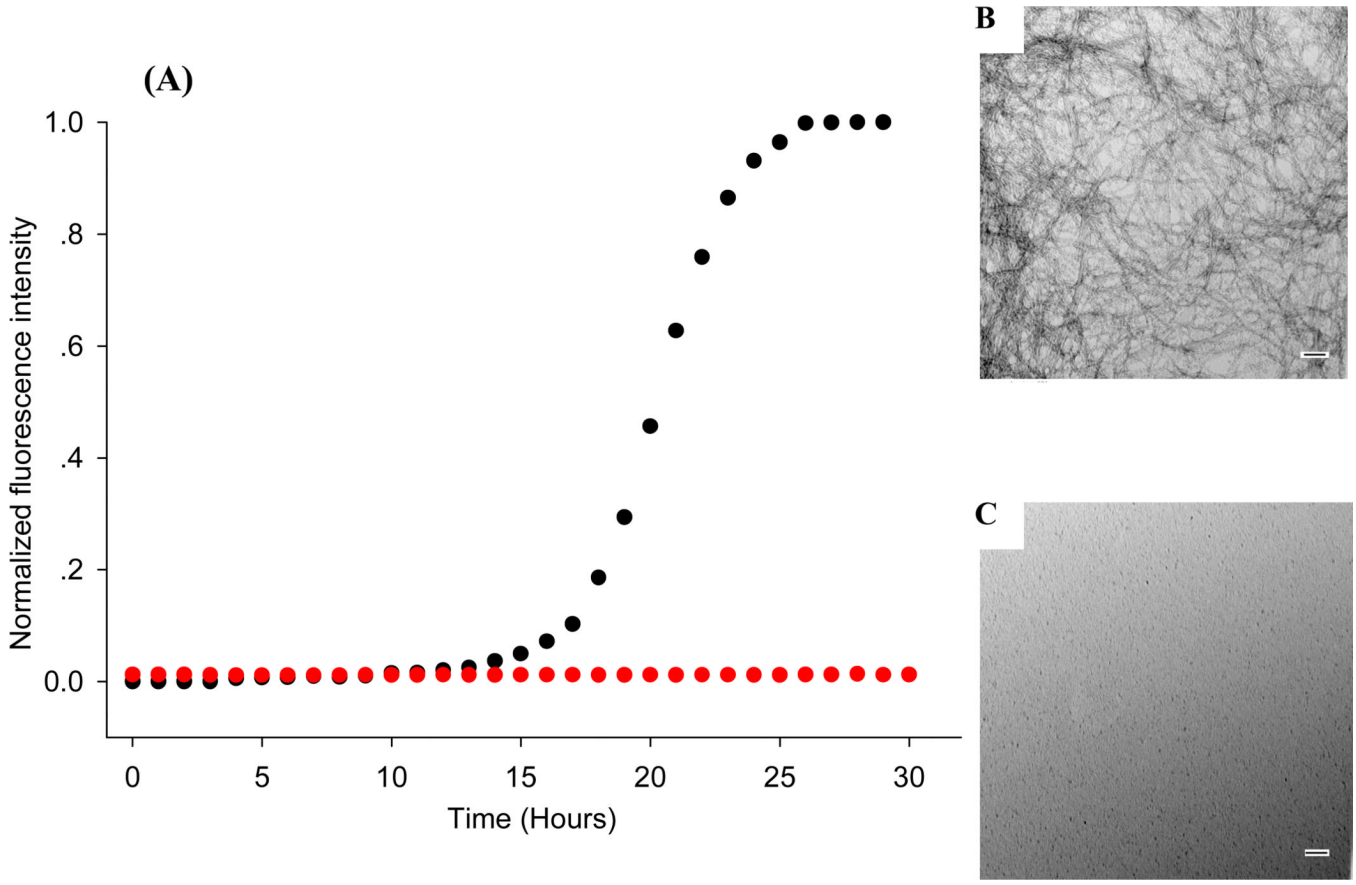

Figure 7.

Interactions with protein amino groups or Cys-2 and Cys-7 are not required for the inhibition of amyloid formation. (A) Inhibition of amyloid formation by the acetylated 8–37 variant of IAPP, $IAPP_{Ac8\text{-}37}$. Thioflavin-T monitored kinetic experiments are shown in the presence (red) and absence of (black) EGCG. TEM images recorded of samples removed after 50 hours are displayed. (B) $IAPP_{Ac8\text{-}37}$ without EGCG. (C) $IAPP_{Ac8\text{-}37}$ with EGCG. Scale bars represent 100 nm. Experiments were conducted at 25°C, pH 7.4, 20 mM Tris-HCl, 32 micromolar thioflavin-T, 16 micromolar IAPP, EGCG when present was at 16 micromolar.

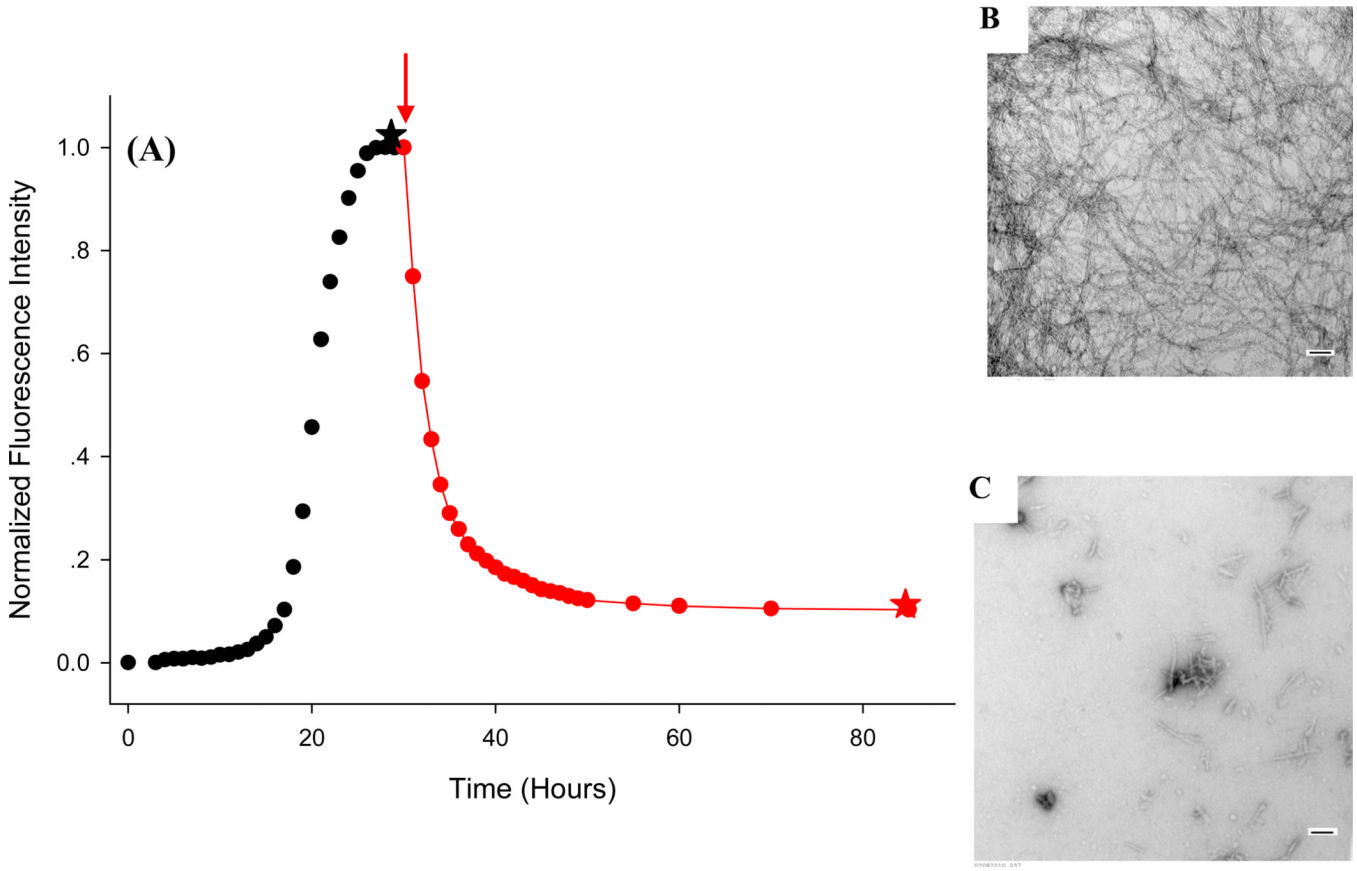

Figure 8.

Interactions with protein amino groups or the disulfide are not required for the effective remodeling of pre-formed IAPP amyloid fibers. Remodleling of $IAPP_{Ac8\text{-}37}$ amyloid fibers by EGCG: (A) Thioflavin-T-monitored experiments: black, $IAPP_{Ac8\text{-}37}$ alone; red, EGCG added at the point indicated by the arrow. (B) TEM image of IAPP before the addition of EGCG, collected from a sample removed at the time point indicated by the black star. (C) TEM image collected after the addition of EGCG. The sample was removed at the time point corresponding to the red star. Scale bars are 100 nm. Experiments were conducted at 25°C, pH 7.4, 20 mM Tris-HCl, 32 micromolar thioflavin-T, 16 micromolar IAPP, EGCG when present was at 16 micromolar.

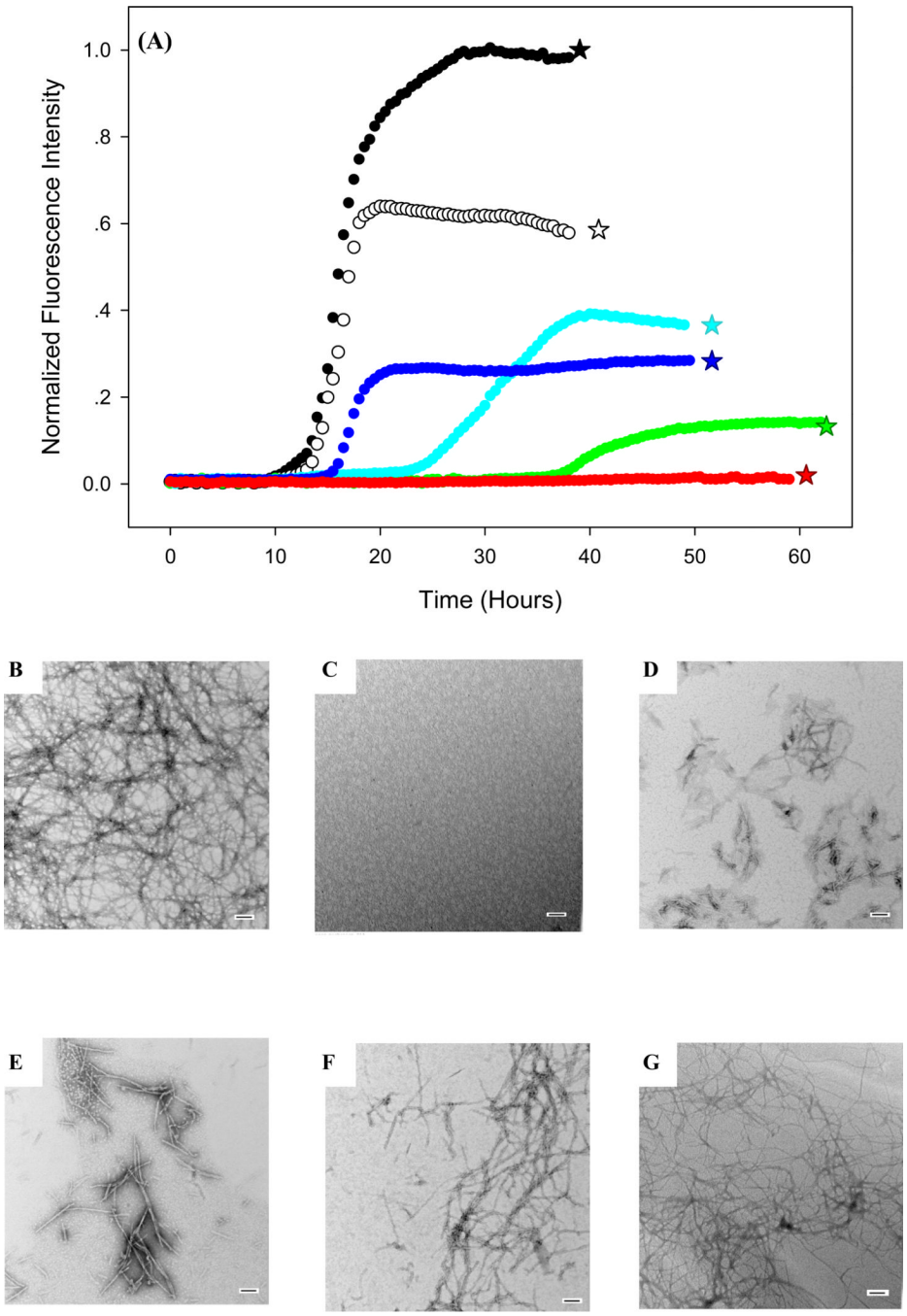

Figure 9.

The gallate ester and the integrity of the tri-hydroxyl phenyl ring are important for the effectiveness of EGCG. (A) Thioflavin-T-monitored kinetic experiments of amyloid formation by wild type IAPP in the presence of various inhibitors. IAPP alone (black); IAPP plus EGCG (red); IAPP plus GCG (green); IAPP plus EGC (blue); IAPP plus ECG (cyan) IAPP plus Epi-Catechin (white). TEM images of IAPP plus flavanols are also shown. The samples were removed at the time point corresponding to the stars. (B) IAPP alone. (C) IAPP plus EGCG. (D) IAPP plus GCG. (E) IAPP plus EGC. (F) IAPP plus ECG. (G) IAPP plus Epi-Catechin. Scale bars are 100 nm. All experiments were conducted at 25°C, pH 7.4,

20 mM Tris-HCl, 32 micromolar thioflavin-T, 0.25% DMSO, 32 micromolar IAPP, EGCG or its derivatives when present was at 32 micromolar.

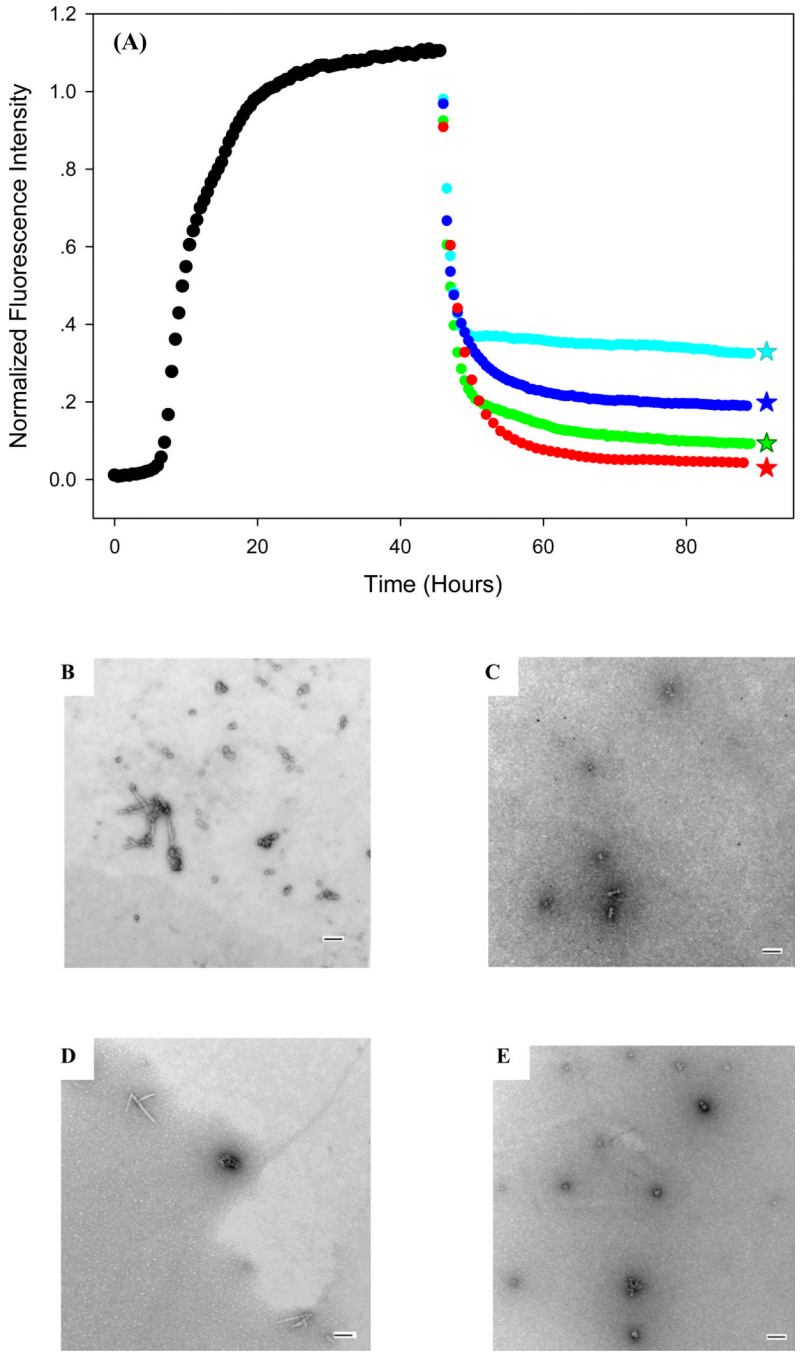

Figure 10.

Remodeling of IAPP amyloid fibers by amyloid inhibitors. (A) Thioflavin-T-monitored experiments are shown. Inhibitors were added at the time point indicated by the arrow. Black, IAPP alone; Red, EGCG; Green, GCG; Blue EGC; Cyan ECG. TEM images collected after addition of flavanols are also shown. The samples were removed at the time point corresponding to the stars. (B) IAPP plus EGCG. (C) IAPP plus GCG. (D) IAPP plus EGC. (E) IAPP plus ECG. Scale bars are 100 nm. Experiments were conducted at 25°C, pH 7.4, 20 mM Tris-HCl, 32 micromolar thioflavin-T, 0.25% DMSO, 32 micromolar IAPP, EGCG or its derivatives when present was at 32 micromolar.